Available online at www.sciencedirect.com
SCIENCE DIRECT®
Mechanics of Materials 36 (2004) 949–958
MECHANICS OF MATERIALS
www.elsevier.com/locate/mechmat

The effective pyroelectric and thermal expansion coefficients of ferroelectric ceramics

JiangYu Li *

Department of Engineering Mechanics, University of Nebraska-Lincoln, W317.5 Nebraska Hall, Lincoln, NE 68588-0526, USA

Received 5 November 2002; received in revised form 13 May 2003

Abstract

We present a micromechanical analysis on the effective pyroelectric and thermal expansion coefficients of ferroelectric ceramics in terms of their microstructural information. The overall behaviors of ferroelectric ceramics are profoundly influenced by the microstructural phenomena, where the macroscopic pyroelectric effect can be induced in an originally isotropic, thus non-pyroelectric ceramic composed of randomly oriented ferroelectric grains through poling, during which the polar axes of grains are switched by the applied electric field or mechanical stress. To analyze these complicated phenomena, we will first establish an exact connection between the effective thermal moduli and the effective electroelastic moduli of ferroelectric ceramics, and then combine the exact connection with the effective medium approximation to provide an estimate on the effective pyroelectric and thermal expansion coefficients of ferroelectric ceramics in terms of the orientation distribution of grains and poling conditions, where the texture evolution as a result of domain switching during poling has been taken into account. Numerical results are presented and good agreements with known theoretical results and some experimental data are observed.

Keywords: Pyroelectricity; Ferroelectricity; Piezoelectricity; Ceramics; Effective moduli

1. Introduction

The crystals having a spontaneous polarization along a unique polar axis are called pyroelectric (Jona and Shirane, 1993), where the spontaneous polarization is dependent on the temperature, and electric charges can be induced on the crystal surface by temperature change. Pyroelectric devices relying on the temperature sensitivity of polarization have received increasing interest in recent years, and have been utilized for various application such as infrared detection, imaging systems, and thermal-medical diagnostics (Cross, 1993).

A ceramic made of pyroelectric grains does not necessarily possess overall pyroelectric effect, because the center-symmetry of randomly oriented ceramics prevents pyroelectric effect at macroscopic scale. If the grains are also ferroelectric, i.e., if the polar axis can be switched by the applied electric field or mechanical stress, then macroscopic pyroelectric effect can be induced in the ceramics through poling, where a high electric field is applied to the ceramic at an elevated

* Tel.: +1-402-4721631; fax: +1-402-4728292.
E-mail address: jli2@unl.edu (J.Y. Li).

0167-6636/$ - see front matter © 2003 Elsevier Ltd. All rights reserved.
doi:10.1016/j.mechmat.2003.05.005

temperature. The microstructural evolution during poling is very complex and involves polarization switching, domain wall movement, intergranular constraint, and microstress generation. The complicated microstructural phenomena obviously have profound influence on the macroscopic pyroelectricity of ceramics, and this work will study the effects of microstructural phenomena at domain and grain levels, including orientation distribution of domains and grains, on the effective pyroelectric and thermal expansion coefficients of ferroelectric ceramics. The texture evolution in ferroelectric ceramics during poling will be taken into account.

Although much effort has been made to understand the effective piezoelectric moduli of ferroelectric ceramics (Dunn, 1995; Nan and Clarke, 1996; Rödel and Kreher, 1999; Li, 2000a), little work has been done to predict the effective thermal moduli of ferroelectric ceramics in terms of their microstructure. Instead, quite a few micromechanical analysis on the effective thermal moduli of piezoelectric composites have been developed (Dunn, 1993a,b; Benveniste, 1994; Chen, 1994a; Qin et al., 1998; Li and Dunn, 1998; Levin et al., 1999; Aboudi, 2001). This is probably because the microstructural phenomena in ferroelectric ceramics are more involved. In this work, we extend the self-consistent approach originally developed for electroelastic moduli (Li, 2000a) to predict the effective pyroelectric and thermal expansion coefficients of ferroelectric ceramics. The analysis shares the same spirit as many works in elastic polycrystals, where an exact connection between the effective thermal moduli and the effective electroelastic moduli is established first (Levin, 1967; Rosen and Hashin, 1970; Hashin, 1984; Schulgasser, 1987; Kreher, 1988; Li, 2000b), and the effective medium approximation is then applied to analyze the local electromechanical fields in ceramics (Walpole, 1969; Willis, 1977; Qiu and Weng, 1991). The recent results on the equilibrium domain configuration in a saturated ferroelectric ceramics have been employed to estimate the effective texture of poled ferroelectric ceramics (Bhattacharya and Li, 2001; Li and Bhattacharya, 2002).

We introduce the basic equation and notation in Section 2, followed by the exact relationships governing the effective constitutive moduli in Section 3. Micromechanics approximation will be introduced in Section 4, and microstructural features such as texture and orientation distribution function (ODF) under various poling conditions are discussed in Section 5. We will then present some numerical results and discussion on the effective pyroelectric and thermal expansion coefficients of ferroelectric ceramics in Section 6. It is demonstrated that the microstructure has important effect on the overall pyroelectric and thermal expansion coefficients of ceramics, and good agreements between numerical results and known theoretical results and some experimental data are observed.

2. Basic equations and notation

We consider the piezoelectric analog of the uncoupled theory of thermoelasticity, where the constitutive equations are given by

$$\begin{aligned} \sigma_{ij} &= L^E_{ijkl}\varepsilon_{kl} + e_{ijk}(-E_k) - \lambda^E_{ij}\theta, \\ D_i &= e_{ikl}\varepsilon_{kl} - \kappa^{\varepsilon}_{ik}(-E_k) - p^{\varepsilon}_i\theta \end{aligned} \tag{1}$$

or its inverse

$$\begin{aligned} \varepsilon_{ij} &= M^D_{ijkl}\sigma_{kl} + g_{ijk}D_k + \alpha^D_{ij}\theta, \\ -E_i &= g_{ikl}\sigma_{kl} - t^{\sigma}_{ik}D_k + \gamma^{\sigma}_i\theta. \end{aligned} \tag{2}$$

In the equations, σ_{ij} and ε_{kl} are stress and strain tensors, respectively; D_i and E_k are electric displacement and electric field, respectively; θ is the temperature change with respect to a reference temperature. The meanings of elastic moduli L^E_{ijkl} and M^D_{ijkl}, piezoelectric coefficients e_{ijk} and g_{ijk}, dielectric constants $\kappa^{\varepsilon}_{ik}$ and t^{σ}_{ik}, thermoelastic constants λ^E_{ij} and α^D_{ij}, and thermoelectric constants p^{ε}_i and γ^{σ}_i are clear from the constitutive equations. We notice that $-E_i$ rather than E_i is used as dependent variable, because it gives us the symmetric moduli matrix which proves to be convenient. We also notice that by choosing different sets of independent variables, other sets of constitutive equations can be obtained. For example, it is easier to measure thermal expansion coefficients $\alpha^E_{ij} = \frac{\partial \varepsilon_{ij}}{\partial \theta}|_{\sigma_{mn},E_m}$ and pyroelectric coefficients

$p_i^\sigma = \frac{\partial D_i}{\partial \theta}|_{\sigma_{mn},E_n}$, and they are related to current moduli by

$$\alpha_{ij}^D = \alpha_{ij}^E - g_{ijk}p_k^\sigma, \quad \gamma_i^\sigma = t_{ij}^\sigma p_j^\sigma. \tag{3}$$

Notice that γ_i^σ is the figure of merit used by a designer to assess the performance of a pyroelectric material for a typical device (Newnham et al., 1978).

To proceed, we adopt the notation introduced by Barnett and Lothe (1975) that treats the elastic and electric variables on an equal footing. It is similar to the conventional indicial notation with the exception that both lowercase and uppercase subscripts are used as indices, where lowercase ones take on the range 1–3, and uppercase ones take on the range 1–4, and repeated uppercase subscripts are summed over 1–4. With this notation, the field variables are expressed as

$$\begin{aligned} \Sigma_{iJ} &= \begin{cases} \sigma_{ij}, & J = 1,2,3, \\ D_i, & J = 4, \end{cases} \\ Z_{Kl} &= \begin{cases} \varepsilon_{kl}, & K = 1,2,3, \\ -E_l, & K = 4, \end{cases} \end{aligned} \tag{4}$$

the electroelastic moduli are expressed as

$$\begin{aligned} G_{iJKl} &= \begin{cases} L_{ijkl}^E, & J,K = 1,2,3, \\ e_{ijl}, & J = 1,2,3,\ K = 4, \\ e_{ikl}, & J = 4,\ K = 1,2,3, \\ -\kappa_{il}^\varepsilon, & J,K = 4, \end{cases} \\ H_{JilK} &= \begin{cases} M_{ijkl}^D, & J,K = 1,2,3, \\ g_{ijl}, & J = 1,2,3,\ K = 4, \\ g_{ikl}, & J = 4,\ K = 1,2,3, \\ -t_{il}^\sigma, & J,K = 4 \end{cases} \end{aligned} \tag{5}$$

and the thermal moduli are expressed as

$$\begin{aligned} \Lambda_{iJ} &= \begin{cases} \lambda_{ij}^E, & J = 1,2,3, \\ p_i^\varepsilon, & J = 4, \end{cases} \\ \Gamma_{Ji} &= \begin{cases} \alpha_{ij}^D, & J = 1,2,3, \\ \gamma_i^\sigma, & J = 4. \end{cases} \end{aligned} \tag{6}$$

As a result, the constitutive equations (1) and (2) can be rewritten as

$$\Sigma_{iJ} = G_{iJKl}Z_{Kl} - \Lambda_{iJ}\theta, \quad Z_{Ji} = H_{JilK}\Sigma_{lK} + \Gamma_{Ji}\theta, \tag{7}$$

where

$$H_{JilK} = G_{lKJi}^{-1}, \quad \Gamma_{Ji} = H_{JilK}\Lambda_{lK}. \tag{8}$$

Finally, we notice the differential constraints on the field variables in terms of the equilibrium equation

$$\Sigma_{iJ,i} = 0, \tag{9}$$

and gradient equation

$$Z_{Ji} = U_{J,i}, \tag{10}$$

with

$$U_J = \begin{cases} u_j, & J = 1,2,3, \\ \phi, & J = 4, \end{cases} \tag{11}$$

where u_i and ϕ are displacement and electric potential, respectively.

3. The effective moduli

Let us now consider a ferroelectric polycrystalline ceramic subjected to a uniform temperature change θ, with linear displacement and electric potential $Z_{Kl}^0 x_l$, or uniform traction and electric displacement $\Sigma_{kL}^0 n_k$ applied at the boundary, where x_l is the position vector and n_k is the outward normal. The polycrystal is composed of grains with certain orientation distribution, each having distinct constitutive moduli in the global coordinate system due to the variation in grains' orientation and grain anisotropy. The constitutive moduli of polycrystalline aggregate, as a result, is heterogenous at microscopic level. This leads to a heterogeneous local electromechanical field in polycrystal at grain level, which depends on Ω, the orientation of individual grains. However, at the macroscopic level the effective constitutive moduli can be defined through the effective constitutive equation if the polycrystal is statistically homogeneous (Nemat-Nasser and Hori, 1999),

$$\begin{aligned} \langle \Sigma_{iJ}(\Omega) \rangle &= G_{iJKl}^* \langle Z_{Kl}(\Omega) \rangle - \Lambda_{iJ}^* \theta, \\ \langle Z_{Kl}(\Omega) \rangle &= H_{KliJ}^* \langle \Sigma_{iJ}(\Omega) \rangle + \Gamma_{Kl}^* \theta, \end{aligned} \tag{12}$$

where $\langle \cdot \rangle$ is used to denote the orientation-averaged quantities in polycrystal, weighted by the orientation distribution function (ODF), which describes the probability of a grain falling into

certain range of orientation. From the averaging theorem (Dunn and Taya, 1993), we have

$$\langle Z_{Kl}(\Omega)\rangle = Z^0_{Kl} \quad \text{or} \quad \langle \Sigma_{iJ}(\Omega)\rangle = \Sigma^0_{iJ}, \tag{13}$$

for specified linear displacement and electric potential or uniform traction and electric displacement at the boundary.

In order to derive the effective constitutive moduli of ferroelectric polycrystals, it is convenient to decompose the electroelastic field in the polycrystal into two parts, one is due to the electromechanical loading (the applied linear displacement and potential $Z^0_{Ji}x_i$ or the applied uniform traction and electric displacement $\Sigma^0_{iJ}n_i$ at the boundary), the loading field I, and the other is due to the temperature change θ, the thermal field II. This decomposition is possible because of the linearity of the constitutive relationships. In light of this decomposition, the effective constitutive equation for loading field and thermal field can be written as

$$\langle \Sigma^{\mathrm{I}}_{iJ}(\Omega)\rangle = G^*_{iJKl}Z^0_{Kl} \quad \text{or} \quad \langle Z^{\mathrm{I}}_{Ji}(\Omega)\rangle = H^*_{JilK}\Sigma^0_{lK} \tag{14}$$

and

$$\langle \Sigma^{\mathrm{II}}_{iJ}(\Omega)\rangle = -\Lambda^*_{iJ}\theta, \quad \langle Z^{\mathrm{II}}_{Ij}(\Omega)\rangle = \Gamma^*_{Ij}\theta, \tag{15}$$

whereas the constitutive equations for individual grains can be written as

$$\begin{aligned} \Sigma^{\mathrm{I}}_{iJ}(\Omega) &= G_{iJKl}(\Omega)Z^{\mathrm{I}}_{Kl}(\Omega),\\ Z^{\mathrm{I}}_{Ji}(\Omega) &= H_{JilK}(\Omega)\Sigma^{\mathrm{I}}_{lK}(\Omega) \end{aligned} \tag{16}$$

and

$$\begin{aligned} \Sigma^{\mathrm{II}}_{iJ}(\Omega) &= G_{iJKl}(\Omega)Z^{\mathrm{II}}_{Kl}(\Omega) - \Gamma_{iJ}(\Omega)\theta,\\ Z^{\mathrm{II}}_{Ji}(\Omega) &= H_{JilK}(\Omega)\Sigma^{\mathrm{II}}_{lK}(\Omega) + \Lambda_{Ji}(\Omega)\theta. \end{aligned} \tag{17}$$

It is noted that at the microscopic level, the thermal field $\Sigma^{\mathrm{II}}_{iJ}(\Omega)$ or $Z^{\mathrm{II}}_{Ji}(\Omega)$ has contribution from both electroelastic field and temperature change, due to the interaction between grains in polycrystals. Because of the linearity, we can introduce the field concentration factors $A_{JiKl}(\Omega)$ and $B_{kLmN}(\Omega)$ defined by

$$\begin{aligned} Z^{\mathrm{I}}_{Ji}(\Omega) &= A_{JiKl}(\Omega)Z^0_{Kl} \quad \text{or}\\ \Sigma^{\mathrm{I}}_{iJ}(\Omega) &= B_{iJlK}(\Omega)\Sigma^0_{lK}, \end{aligned} \tag{18}$$

and thermal concentration factors $a_{Ji}(\Omega)$ and $b_{iJ}(\Omega)$ defined by

$$Z^{\mathrm{II}}_{Ji}(\Omega) = a_{Ji}(\Omega)\theta, \quad \Sigma^{\mathrm{II}}_{iJ}(\Omega) = b_{iJ}(\Omega)\theta, \tag{19}$$

which leads to

$$\begin{aligned} G^*_{iJKl} &= \langle G_{iJNm}(\Omega)A_{NmKl}(\Omega)\rangle,\\ H^*_{JilK} &= \langle H_{JimN}(\Omega)B_{mNlK}(\Omega)\rangle \end{aligned} \tag{20}$$

and

$$\begin{aligned} \Lambda^*_{iJ} &= \langle -G_{iJNm}(\Omega)a_{Nm}(\Omega) + \Lambda_{iJ}(\Omega)\rangle,\\ \Gamma^*_{Ji} &= \langle H_{JimN}(\Omega)b_{mN}(\Omega) + \Gamma_{Ji}(\Omega)\rangle. \end{aligned} \tag{21}$$

The determination of the effective constitutive moduli of polycrystal is thus dependent on the determination of field and thermal concentration factors as functions of grains' orientation, and their orientational averaging. We also notice from the averaging theorem that

$$\langle A_{iJlK}(\Omega)\rangle = I_{iJlK}, \quad \langle B_{JiKl}(\Omega)\rangle = I_{JiKl} \tag{22}$$

and

$$\langle a_{Ji}(\Omega)\rangle = 0, \quad \langle b_{iJ}(\Omega)\rangle = 0, \tag{23}$$

with

$$I_{iJlK} = I_{JiKl} = \begin{cases} i_{ijkl}, & J,K = 1,2,3,\\ 0, & J = 1,2,3, K = 4,\\ 0, & J = 4, K = 1,2,3,\\ \delta_{il}, & J,K = 4, \end{cases} \tag{24}$$

where i_{ijkl} is the forth-order unit tensor, and δ_{km} is the Kronecker delta.

It is also possible to determine the effective thermal moduli of polycrystals using field concentration factors instead of thermal concentration factors. To this end, we recall the generalized Hill condition for piezoelectric solids (Li and Dunn, 1999),

$$\langle \Sigma_{iJ}(\Omega)Z_{Ji}(\Omega)\rangle = \langle \Sigma_{iJ}(\Omega)\rangle\langle Z_{Ji}(\Omega)\rangle, \tag{25}$$

which is valid for uniform traction and electric displacement or linear displacement and electrical potential boundary condition. The electromechanical fields Σ_{iJ} and Z_{Ji} do not need to be connected by certain constitutive equations. Now consider the loading field Z^{I}_{Ji} due to the linear elastic displacement and potential boundary condition, and thermal field $\Sigma^{\mathrm{II}}_{iJ}$ due to the temperature change, we have

$$\left\langle \Sigma^{\mathrm{II}}_{iJ}(\Omega) Z^{\mathrm{I}}_{Ji}(\Omega) \right\rangle = \left\langle \Sigma^{\mathrm{II}}_{iJ}(\Omega) \right\rangle Z^{0}_{Ji} = -\Lambda^{*}_{iJ}\theta Z^{0}_{Ji} \tag{26}$$

due to the generalized Hill condition. The left hand side of Eq. (26) can be written as

$$\begin{aligned}\left\langle \Sigma^{\mathrm{II}}_{iJ}(\Omega) Z^{\mathrm{I}}_{Ji}(\Omega) \right\rangle &= \left\langle (G_{iJKl}(\Omega) Z^{\mathrm{II}}_{Kl}(\Omega) \right. \\ &\quad \left. - \Lambda_{iJ}(\Omega)\theta) Z^{\mathrm{I}}_{Ji}(\Omega) \right\rangle \\ &= \left\langle \Sigma^{\mathrm{I}}_{lK}(\Omega) Z^{\mathrm{II}}_{Kl}(\Omega) \right\rangle \\ &\quad - \left\langle \Lambda_{iJ}(\Omega) Z^{\mathrm{I}}_{Ji}(\Omega)\theta \right\rangle \\ &= -\left\langle \Lambda_{iJ}(\Omega) Z^{\mathrm{I}}_{Ji}(\Omega)\theta \right\rangle \\ &= -\left\langle \Lambda_{iJ}(\Omega) A_{JiKl}(\Omega) Z^{0}_{Kl}\theta \right\rangle. \end{aligned} \tag{27}$$

In the derivation, we have used the symmetry of G_{iJKl} and the fact that $\langle Z^{\mathrm{II}}_{Ji} \rangle = 0$ under the specified boundary condition. Combining Eqs. (26) and (27), we obtain

$$\Lambda^{*}_{iJ} = \langle A_{KlJi}(\Omega) \Lambda_{lK}(\Omega) \rangle. \tag{28}$$

A similar manipulation for the applied traction and electric displacement boundary condition yields

$$\Gamma^{*}_{Ji} = \langle B_{lKiJ}(\Omega) \Gamma_{Kl}(\Omega) \rangle. \tag{29}$$

Thus the effective thermal moduli can be determined from either thermal concentration factors or field concentration factors. Notice that in general the concentration factors A_{JiKl} and B_{iJlK} do not have diagonal symmetry.

4. The micromechanics approximations

Up to Eq. (29) the derivation is rigorous under the assumption of macroscopic homogeneity. To carry out the analysis further, we need to make approximations regarding the microstructural field distribution in the polycrystal, and micromechanics approach is appropriate. In this paper we rely the determination of the effective thermal moduli on the field concentration factors, i.e., Eqs. (28) and (29). The key step in the prediction of the effective moduli thus is the determination of the field concentration factor A_{JiKl} and B_{iJlK}. To this end we adopt a self-consistent approach suitable for piezoelectric polycrystals. The essence of self-consistent approach is using the electromechanical field in a single grain embedded in a matrix with yet to be determined uniform effective moduli to simulate the electromechanical field in a grain at a particular orientation in a ceramic. This approximation leads to

$$A_{JiKl}(\Omega) = A^{dil}_{JiNm}(\Omega) \langle A^{dil}_{KlNm}(\Omega) \rangle^{-1} \tag{30}$$

with

$$A^{dil}_{JiKl}(\Omega) = [I_{KlJi} + S_{KlMn}(\Omega) H^{*}_{MnoP} (G_{oPJi}(\Omega) - G^{*}_{oPJi})]^{-1}, \tag{31}$$

derived from the single inclusion solution, where S_{KlMn} are the piezoelectric Eshelby tensors which are functions of grain shape, orientation, and the electromechanical moduli of matrix (Dunn and Taya, 1993). In general, Eq. (30) need to be solved numerically by iteration, which usually converges pretty fast. Notice that the interaction between grains is taken into account in the self-consistent approach through the effective medium approximation, and the normalization condition (22) is automatically satisfied. A simpler approximation would assume

$$A_{JiKl} = I_{JiKl}, \quad B_{iJlK} = I_{iJlK}, \tag{32}$$

which is analog of Voigt and Reuss averages for elastic materials. The Voigt and Reuss averages usually do not predict the effective moduli of polycrystal accurately when the crystalline anisotropy is strong.

5. Orientation distribution function and texture

The issue remains on how to characterize the microstructure of ferroelectric ceramics. The orientation of grains in a ferroelectric ceramic could be described by θ_{g}, the angle between the global poling axis of ceramic and the local crystallographical axis of grains. Within each grains there are numerous domains whose orientation can be described by $\theta_{\mathrm{d}}(\theta_{\mathrm{g}})$, the angle between the polarization direction of domains and the poling direction of ceramic, which depends on the grain's orientation θ_{g} through crystallographic constraints. The number of possible domain orientations within a particular grain is governed by crystallography. For example, in tetragonal

system, six orientations are available while for rhombohedral system, there are eight possible domain orientations in each grain. The statistical distribution of θ_g and θ_d are then described by the orientation distribution function (ODF) $W^g(\theta_g)$ and $W^d(\theta_d)$, which gives the probability of finding a grain or a domain in a particular orientation. In the as-processed states, individual grains are randomly oriented in ceramics, so that $W^g(\theta_g)$ and $W^d(\theta_d)$ are uniform throughout the ceramics and independent on θ_g and θ_d, and the ceramic is isotropic and non-pyroelectric. The poling process, where a high electric field is applied to ceramics at elevated temperature, tends to realign the polarization directions of domains as closely as possible to the applied field, thus effectively changes the orientation distribution of domains, $W^d(\theta_d)$, but does not change the orientation distribution of grains, $W^g(\theta_g)$. For ceramics composed of randomly oriented tetragonal grains, if all domains are switched to be as closely as possible to the poling direction in a 'fully poled' state, $W^d(\theta_d)$ would be uniform for $\theta_d \in [0, \pi/4]$ and zero elsewhere. If all 180° domains are switched and none of the 90° domains are switched in a 'partially poled' state, the corresponding ODF for domains is uniform for $\theta_d \in [0, \pi/2]$ and zero elsewhere. The actual orientation distribution of domains in a poled ferroelectric ceramic is rather difficult to determine, but can be fairly well approximated by Taylor texture derived from Taylor estimate (Li and Bhattacharya, 2002),

$$W(\theta_d) = \frac{1 + \cos\theta_d}{2}. \tag{33}$$

This expression is derived based on the assumption that strain and polarization caused by the domain switching is uniform in polycrystal, which leads to accurate predictions on the saturation strain and polarization in ferroelectric ceramics. In the Taylor estimate, none of 90° domains are switched, and only part of 180° domains are switched. As a result, the 'fully poled' ceramics have most domain switched, and Taylor estimated ceramics have least domain switched. The change in orientation distribution of domains leads to macroscopic pyroelectricity in ceramics, which we analyze here.

In addition to the texture evolution due to the domain switching induced by poling, the pre-poling texture of ceramics also have important influences on the overall behaviors of ceramics. To analyze this effect we adopt Gaussian distribution function as ODF of grains for pre-poling texture,

$$W(\theta_g) = \frac{1}{\mu\sqrt{2\pi}} \exp\left(-\frac{\theta_g^2}{2\mu^2}\right), \tag{34}$$

which can be used to simulate a wide range of texture in piezoelectric polycrystals by adjusting the parameter μ. For example $\mu \to \infty$ represents random texture in unpoled isotropic ceramics, and $\mu \to 0$ represents fiber texture in thin films. The ODF for various textures in ferroelectric ceramics are summarized in Table 1. They need to be normalized to be used in the orientational averaging of any physical quantities of polycrystals.

6. Numerical results and discussion

With ODF given, we developed a numerical algorithm to carry out the orientational averaging in Eqs. (28) and (29) by numerical integration using Gaussian quadrature method (Press et al., 1992), where the integral is approximated by the sum of its integrand values at a set of points called abscissas weighted by weighting coefficients. We carried out the numerical calculations for tetragonal barium titanate ceramics, with materials data of single domain single crystal listed in Table 2. The electroelastic moduli are obtained from Zgonik et al. (1994), and the thermal moduli are

Table 1
Orientation distribution function of polycrystals with different textures and poling conditions

Texture	Random	Random	Gaussian	Taylor
Poling	Full	Partial	Partial	Partial
$W(\theta)$	1 ($\theta \in [0, \pi/4]$)	1 ($\theta \in [0, \pi/2]$)	$\frac{1}{\mu\sqrt{2\pi}}\exp\left(-\frac{\theta^2}{2\mu^2}\right)$	$\frac{1+\cos\theta}{2}$

Table 2
The thermoelectroelastic moduli of barium titanate single crystal (Zgonik et al., 1994; Jona and Shirane, 1993)

L^E_{11}	L^E_{12}	L^E_{13}	L^E_{33}	L^E_{44}	L^E_{66}	e_{31}	e_{33}	e_{15}	κ^ε_{11}	κ^ε_{33}	α^E_{11}	α^E_{33}	p^σ_3
222	108	111	151	61	134	−0.7	6.7	34.2	2200	56	11.8	−18.5	5.53

L: GPA, e: C/m^2, κ: κ_0, α: $\times 10^{-6}$, p: $\times 10^{-4}$ C/m^2 K.

estimated from figures in (Jona and Shirane, 1993). In the calculation, the grain is assumed to be spherical.

We first demonstrate the effect of poling on the effective thermal moduli. The effective pyroelectric and thermal expansion coefficients are given in Figs. 1 and 2 in terms of various degree of poling, and are compared with experiment measurement. It is clear that domain switching tends to increase the effective pyroelectric coefficient, and Taylor estimate on pyroelectric coefficient agrees with experiment measurement well, which suggests that only some 180° domains and few of 90° domains are switched during poling. This is consistent with well known observation that 90° domain switching is much harder than 180° domain switching, which does not involve transformation strain as 90° domain switching does. It is also observed that 'fully poled' ceramic has highest α^D_{11}, while 'partially poled' ceramic has highest α^D_{33}. It suggests that 90° domain switching tends to decrease α^D_{33} and increase α^D_{11}, consistent with the anisotropy of thermal expansion coefficients of single crystals. Poor agreement with experiment measurement on thermal expansion coefficients are observed. This is at least partly due to the lacking of accurate single crystal data.

We then demonstrate the effect of textures on the effective pyroelectric and thermal expansion coefficients using Gaussian distribution function as ODF. The effective pyroelectric and thermal expansion coefficients in terms of Gaussian distribution parameter μ predicted by the self-consistent approach and Voigt–Reuss averages are given in Figs. 3 and 4. We also give the effective piezoelectric coefficients in Fig. 5 as a comparison. When μ approaches zero, which implies that the ceramics posses fiber texture, the predictions of pyroelectric coefficients, piezoelectric coefficients, and thermal expansion coefficients given by the

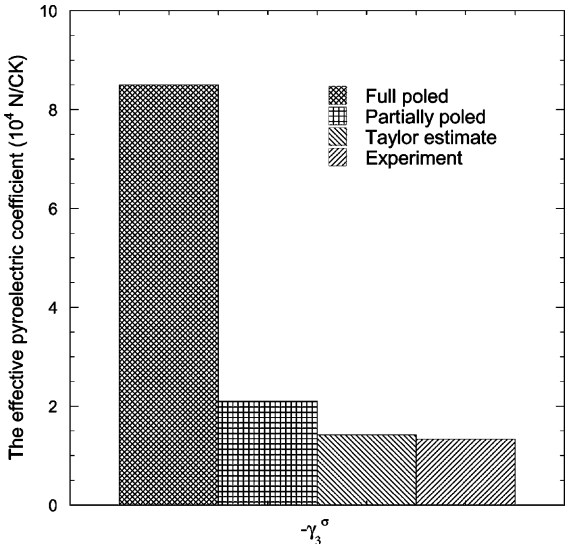

Fig. 1. The effective pyroelectric coefficient for various extents of poling; experiment data are from Dunn (1993a,b).

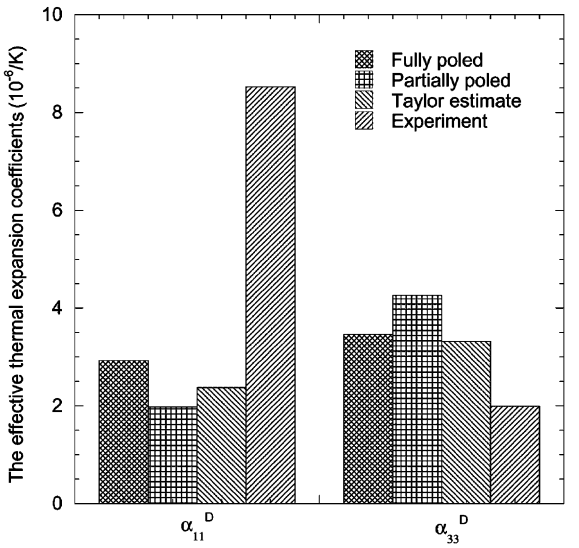

Fig. 2. The effective thermal expansion coefficients for various extents of poling; experiment data are from Dunn (1993a,b).

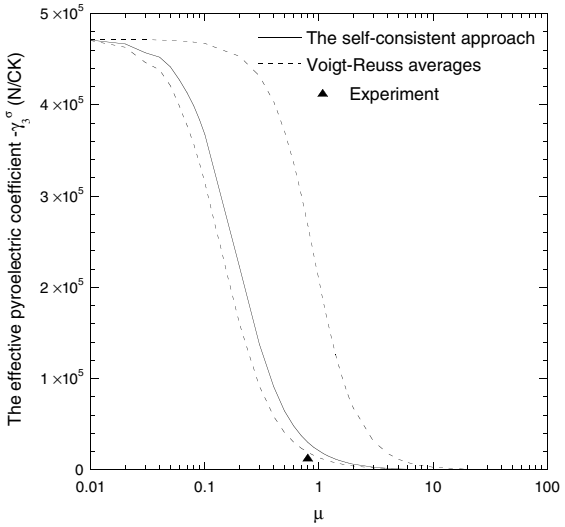

Fig. 3. The effective pyroelectric coefficient for various textures; experiment data are from Dunn (1993a,b).

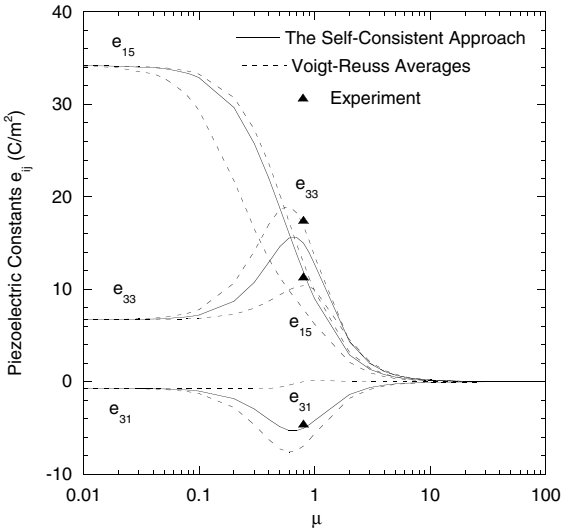

Fig. 5. The effective piezoelectric coefficients for various textures; experiment data are from Dunn (1993a,b).

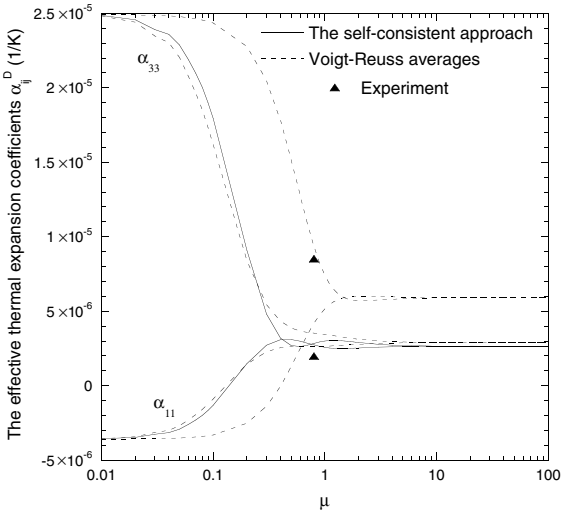

Fig. 4. The effective thermal expansion coefficients for various textures; experiment data are from Dunn (1993a,b).

self-consistent approach and Voigt–Reuss averages all converge to the single crystal values, consistent with the exact relationship obtained by Li et al. (1999). When μ approach infinity, which implies that the ceramic is isotropic, the effective pyroelectric and piezoelectric coefficients become zero, and α_{33} converges to α_{11}, as expected. The effective pyroelectric coefficient decreases with the increase of μ monotonically, while the variations of thermal expansion coefficients and piezoelectric constants are not monotonic. It is also observed that the predictions between the self-consistent approach and Voigt average ($\mathbf{A} = \mathbf{I}$) are close to each other. Reasonably good agreement with experiment measurement is observed near $\mu = 0.8$ for the effective piezoelectric, pyroelectric, and thermal expansion coefficients, which suggests that the ODF of poled barium titanate ceramics can be approximated by the Gaussian distribution function with $\mu = 0.8$.

Finally we would like to point out that for a pure elastic polycrystal, there are exact relationships between the effective thermal expansion coefficients and the effective elastic moduli (Schulgasser, 1987). We are unable to establish similar relationships for ferroelectric ceramics, except in some special situations. For example, the exact relationships have been established by Benveniste (1994) and Li et al. (1999) for piezoelectric polycrystals with fiber texture, and by Chen (1994b) for certain specific crystal symmetries.

7. Concluding remarks

We have applied the self-consistent approach to predict the effective pyroelectric and thermal expansion coefficients of ferroelectric ceramics, taking into account the texture change due to domain switching during poling. The variations of thermal moduli with respect to the poling and texture have been demonstrated, and good agreements with theoretical results and experiment measurements have been observed.

Acknowledgements

Financial support by the Layman Award from Research Council, University of Nebraska-Lincoln and NSF Nebraska EPSCoR Type II Grant is gratefully acknowledged.

References

Aboudi, J., 2001. Micromechanical analysis of fully coupled electro-magneto-thermo-elastic multiphase composites. Smart Mater. Struct. 10, 867–877.

Barnett, D.M., Lothe, J., 1975. Dislocations and line charges in anisotropic piezoelectric insulators. Phys. Stat. Sol. B 67, 105–111.

Bhattacharya, K., Li, J.Y., 2001. Domain patterns, texture and macroscopic electromechanical behavior of ferroelectrics. In: Proceedings of The 11th Williamsburg Workshop on Fundamental Physics of Ferroelectrics, AIP Conference Proceedings 582, pp. 72–81.

Benveniste, Y., 1994. Exact Connections between polycrystal and crystal properties in 2-dimensional polycrystalline aggregates. Proc. R. Soc. London A 447, 1–22.

Chen, T., 1994a. Micromechanical estimates of the overall thermoelectroelastic moduli of multiphase fibrous composites. Int. J. Solids Struct. 31, 3099–3111.

Chen, T., 1994b. Effective thermal expansion of piezoelectric polycrystals. J. Mater. Sci. Lett. 13, 1175–1176.

Cross, E.L., 1993. Ferroelectric ceramics: tailoring properties for specific applications. In: Setter, N., Colla, E.L. (Eds.), Ferroelectric Ceramics. Birkhäuser Verlag, Berlin, pp. 1–85.

Dunn, M.L., 1993a. Micromechanics of coupled electroelastic composites—effective thermal-expansion and pyroelectric coefficients. J. Appl. Phys. 73, 5131–5140.

Dunn, M.L., 1993b. Exact relations between the thermoelectroelastic moduli of heterogeneous materials. Proc. R. Soc. London A. 441, 549–557.

Dunn, M.L., 1995. Effects of grain shape anisotropy, property, and microcracks on the elastic and dielectric-constants of polycrystalline piezoelectric ceramics. J. Appl. Phys. 78, 1533–1541.

Dunn, M.L., Taya, M., 1993. An analysis of piezoelectric composite-materials containing ellipsoidal inhomogeneities. Proc. R. Soc. London A. 443, 265–287.

Hashin, Z., 1984. Thermal expansion of polycrystalline aggregates. I. Exact results. J. Mech. Phys. Solids 32, 149–157.

Jona, F., Shirane, G., 1993. Ferroelectric Crystals. Dover Publications, Inc., New York.

Kreher, W.S., 1988. Internal stresses and relations between effective thermoelastic properties of stochastic solids—some exact solutions. Z. Angew. Math. Mech. 68, 147–154.

Levin, V.M., 1967. On the coefficients of thermal expansion of heterogeneous materials. Mekhanika Tverdogo Tela 2, 88–94.

Levin, V.M., Rakovskaja, M.I., Kreher, W.S., 1999. The effective thermoelectroelastic properties of microinhomogeneous materials. Int. J. Solids Struct. 36, 2683–2705.

Li, J.Y., 2000a. The effective electroelastic moduli of textured piezoelectric polycrystalline aggregates. J. Mech. Phys. Solids 48, 529–552.

Li, J.Y., 2000b. Thermoelastic behavior of composites with functionally graded interphase: a multi-inclusion model. Int. J. Solids Struct. 37, 5579–5597.

Li, J.Y., Bhattacharya, K., 2002. A mesoscopic electromechanical theory of ferroelectric films ceramics. In: Fundamental Physics of Ferroelectrics 2002, Proceedings of Workshop on Fundamental Physics of Ferroelectrics AIP Conference Proceedings 626, pp. 224–231.

Li, J.Y., Dunn, M.L., 1998. Micromechanics of magnetoelectroelastic composites: average fields and effective behavior. J. Intell. Mater. Syst. Struct. 9, 404–416.

Li, J.Y., Dunn, M.L., 1999. Analysis of microstructural fields in heterogeneous piezoelectric solids. Int. J. Eng. Sci. 37, 665–685.

Li, J.Y., Dunn, M.L., Ledbetter, H., 1999. Thermoelectroelastic moduli of textured piezoelectric polycrystals: exact solutions and bounds for film textures. J. Appl. Phys. 86, 4626–4634.

Nan, C.W., Clarke, D.R., 1996. Piezoelectric moduli of piezoelectric ceramics. J. Am. Ceram. Soc. 79, 2563–2566.

Nemat-Nasser, S., Hori, M., 1999. Micromechanics: Overall Properties of Heterogenous Solids, second ed. Elsevier Science Publishers, North-Holland.

Newnham, R.E., Skinner, D.P., Cross, L.E., 1978. Connectivity and piezoelectric–pyroelectric composites. Mater. Res. Bull. 13, 525–536.

Press, W.H., Teukolsky, S.A., Vetterling, W.T., Flannery, B.P., 1992. Numerical Recipes in FORTRAN, second ed. Cambridge University Press, Cambridge, UK.

Qin, Q.H., Mai, Y.W., Yu, S.W., 1998. Effective moduli for thermopiezoelectric materials with microcracks. Int. J. Fract. 91, 359–371.

Qiu, Y.P., Weng, G.J., 1991. Elastic-constants of a polycrystal with transversely isotropic grains, and the influence of precipitates. Mech. Mater. 12, 1–15.

Rödel, J., Kreher, W.S., 1999. Effective properties of polycrystalline piezoelectric ceramics. J. Phys. IV 9, 239–247.

Rosen, B.W., Hashin, Z., 1970. Effective thermal expansion coefficient and specific heats of composite materials. Int. J. Eng. Sci. 8, 157–173.

Schulgasser, K., 1987. Thermal expansion of polycrystalline aggregates with texture. J. Mech. Phys. Solids 35, 35–42.

Walpole, L.J., 1969. On the overall elastic moduli of composite materials. J. Mech. Phys. Solids 17, 235–251.

Willis, J.R., 1977. Bounds and self-consistent estimates for the overall properties of anisotropic composites. J. Mech. Phys. Solids 25, 185–202.

Zgonik, M., Bernasconi, P., Duelli, M., Schlesser, R., Günter, P., Garrett, M., Rytz, D., Zhu, Y., Wu, X., 1994. Dielectric, elastic, piezoelectric, electrooptic, and elasto-optic tensors of BaTiO3 crystals. Phys. Rev. B. 50, 5941–5949.